

X-RAY TRIPLE RINGS AROUND THE M87 JETS IN THE CENTRAL VIRGO CLUSTER

HUA FENG¹, SHUANG-NAN ZHANG^{2,5}, YU-QING LOU^{2,6,7} AND TI-PEI LI^{2,4}

(Received 2003 December 17)
Draft version August 26, 2017

ABSTRACT

The *Chandra* X-ray data of the central Virgo cluster are re-examined to reveal a triple-ring structure around the galaxy M87, reminiscent of the spectacular triple-ring pattern of the SN1987A in the Large Magellanic Cloud (LMC). In the sky plane, the two apparent smaller ellipses are roughly aligned along the M87 jets; the larger ring centers at the M87 nucleus and is likely a circle roughly perpendicular to the M87 jet. Certain similarities of these two triple-ring structures might hint at similar processes that operate in these two systems with entirely different sizes and mass scales. We suspect that a major merging event of two galaxies with nuclear supermassive black holes (SMBHs) might create such a triple-ring structure and drove acoustic and internal gravity waves far and near. The M87 jets are perhaps powered by a spinning SMBH resulting from this catastrophic merging event.

Subject headings: X-rays: galaxies: clusters — galaxies: structure — galaxies: individual (M87) — galaxies: clusters: individual (Virgo)

1. INTRODUCTION

Many similar astrophysical phenomena happen on totally different spatial and temporal scales or energy and mass scales. Examples include collimated jets from active galactic nuclei (AGNs) containing SMBHs (Begelman 2003), from microquasars containing stellar mass black holes (Mirabel & Rodriguez 1999) and from young stellar objects (Ray et al. 1996); dynamical roles of waves in spiral galaxies (Lin & Shu 1964; Fan & Lou 1996; Lou & Fan 1998), in planetary rings (Goldreich & Tremaine 1978) and in galaxy clusters (Fabian et al. 2003a); similar high-temperature atmospheres of the Sun and of stellar mass black hole systems (Zhang et al. 2000); similar gamma-ray flashes and bursts from explosions of perhaps massive stars at cosmological distances (Mészáros 2001), from solar flares (Haisch et al. 1991) and from the Earth’s atmosphere (Fishman et al. 1994; Feng et al. 2002). We report here the detection of an X-ray triple-ring structure in the core of the Virgo galaxy cluster, most likely associated with the AGN of the galaxy M87 (NGC 4486) and its powerful jet. This triple-ring structure is reminiscent of the spectacular triple-ring pattern of the supernova 1987A in the LMC (Burrows 1995).

M87 is an active galaxy with relativistic jets in the central Virgo cluster. The X-ray morphology and spectroscopy of the Virgo cluster have been studied previously using data from *Chandra* (Young et al. 2002) and *XMM-Newton* (Böhringer et al. 2001; Belsole et al.

2001). Combining *Chandra*, *XMM* and *ROSAT* data, Forman et al. (2004, hereafter F04) studied the Virgo cluster on various scales to identify cooling flow quenching by an AGN energy input. They noticed two prolate features around the M87 jet and counter jet, and referred to them as “cavities” caused by plasma expansions.

In this Letter, we re-analyze the *Chandra* data and focus on the core region around M87. Two smaller ring structures are identified to encircle the “cavities” noticed by F04; a third larger ring centers at the M87 nucleus. We adopt the distance to M87 as ~ 16 Mpc with $1''$ for ~ 78 pc in the image (Whitmore et al. 1995).

2. DATA ACQUISITION AND ANALYSIS

We process the data of two observations (Obs-ID 2707 and 352) pointed at M87 in the central Virgo cluster by the ACIS-S (Advanced CCD Imaging Spectrometer Spectroscopic array) instrument aboard NASA’s *Chandra X-ray Observatory* for a total effective exposure of 119.2 ks. The data are screened for flares where count rates are at least $3\text{-}\sigma$ away from the mean rate in the S1 chip for 2.5–6.0 keV. The exposures before/after screening are 98.7/89.5 ks for Obs-ID 2707 and 37.7/29.7 ks for Obs-ID 352. These two screened data sets are merged using the *merge_all* script in *CIAO* 3.0.1, and further corrected with an exposure map. Another two long observations of M87 (Obs-ID 3717 and 1808) are not included for analysis because of serious flare contamination.

We avoid the over-brightness of M87 and the jet by extracting the normalized brightness in the range $[0, 8\%]$ and renormalizing linearly to $[0, 1]$, i.e., let B_1 and B_2 be the brightness maps before and after the adjustment, we take $0 \leq B_1 \leq 0.08$ from a normalized brightness map and renormalize it with $B_2 = B_1/0.08$. The 0.5–2.5 keV image of the central Virgo cluster is displayed in Figure 1a by a Gaussian smoothing of $1.5''$ FWHM. To reveal structures of smaller scales in the image, we apply an unsharp mask. A smoothed image G is obtained by convoluting the raw image I with a Gaussian function. The sharpened image U is a weighted subtraction of I and G , viz. $U = I + a(I - G)$ where a is a constant. By trials, we choose a Gaussian function of $15''$

¹ Department of Engineering Physics and Center for Astrophysics, Tsinghua University, Beijing 100084, China

² Physics Department and Center for Astrophysics, Tsinghua University, Beijing 100084, China

³ Physics Department, University of Alabama in Huntsville, Huntsville, AL 35899, USA

⁴ Laboratory for Particle Astrophysics, Institute of High Energy Physics, Chinese Academy of Sciences, Beijing 100039, China

⁵ Space Science Laboratory, NASA Marshall Space Flight Center, SD50, Huntsville, AL 35812, USA

⁶ Department of Astronomy and Astrophysics, The University of Chicago, 5640 South Ellis Avenue, IL 60637, USA

⁷ National Astronomical Observatories, Chinese Academy of Sciences, A20, Datun Road, Beijing 100012, China

TABLE 1
FITTING PARAMETERS AND ORIENTATIONS OF THE TRIPLE RINGS¹

object	projected ellipses			reconstructed rings			
	center (RA, Dec) ($^{\circ}$)	a (kpc)	b (kpc)	θ ($^{\circ}$)	α ($^{\circ}$)	Φ ($^{\circ}$)	Φ' ($^{\circ}$)
ring 1	187.7021, 12.3920	1.9	1.1	76	55	61	55
ring 2	187.7100, 12.3901	1.5	1.3	70	30	51	33
ring 3	187.7059, 12.3916	2.5	2.0	-10	37	9	22
nucleus	187.7059, 12.3911
jet	70	43	0	0

¹a: semi major axis; b: semi minor axis; θ : Angle from the major axis (or M87 jet direction) to the local hour circle line; α : angle from the ring normal (first 3 rows) or M87 jet direction (the last row) to the LOS; Φ : angle between the ring normal and the M87 jet (43° to LOS); Φ' : same with Φ but taken the jet orientation as 15° to LOS.

FWHM with $a = 500\%$. The resulting image of Figure 1b is obtained by smoothing the sharpened image with a Gaussian function of $1.5''$ FWHM and by adjusting the contrast to enhance visibility of the triple-ring feature; the contrast enhancement is done by displaying only the image within the brightness range of 15.5–24%, i.e., 1.24–1.92% in the original image.

For spectra along the rings, a hardness ratio map is shown in Figure 2 for the central Virgo cluster where the hardness ratio is defined as $H = (c_2 - c_1)/(c_2 + c_1)$ with c_1 and c_2 for photon counts in the lower and higher energy bands, respectively (Li 2001). We select 0.5–1.0 keV and 1.0–2.5 keV as the lower and higher bands. The images are smoothed with a $2''$ FWHM Gaussian function before creating a hardness ratio map in Figure 2.

3. THE TRIPLE-RING STRUCTURE

Two nested X-ray ellipses (dashed lines marked as ring 1 and 2 in Figure 1b) are revealed around the M87 jets. A third larger ellipse can be partially seen (dashed line marked as ring 3 in Figure 1b). The reality of ring 1 and 2 is evident by Figure 1b. Besides the northern and southern diffuse arcs for the initial identification of ring 3, the ring also passes through eight bright X-ray knots (marked by small open arrows) that lend further support for its reality. The X-ray morphology of the Virgo cluster is fairly complex with structures on scales from $\sim 1 - 50$ kpc (F04). We mainly focus on the triple-ring structure.

Each presumed circular ring fits a projected ellipse using five parameters (see Table 1), viz., the right ascension (RA) and declination (Dec), semi major and minor axes, and the inclination angle of the semi major axis to the local hour circle line. Because the three X-ray rings can not be readily recognized by our software, errors in these fitting parameters are estimated empirically. We note that position uncertainties are $\lesssim 1 - 2''$ (~ 0.1 kpc) and angular uncertainties are $\lesssim 5^{\circ}$.

It is possible that the observed ellipses are projections of circular rings in the sky plane. We reconstruct 3-D orientations of the three circular rings. The jet orientation may be taken as either 43° (Biretta et al. 1995) relative to the line of sight (LOS) away from us or more likely 15° (within 19° as inferred by Biretta et al. 1999). The angle of the projected jet to the local hour circle line is $\sim 70^{\circ}$ (Figure 1). Thus, the angle Φ (see Table 1) of the

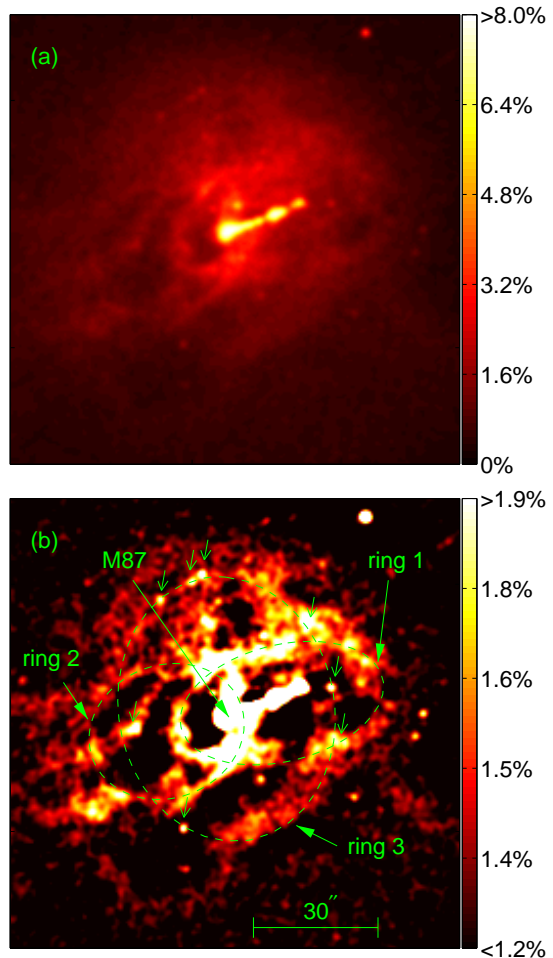


FIG. 1.— Two *Chandra* 0.5–2.5 keV X-ray images of the central Virgo cluster with color bars indicating the fractional flux. (a) — the core image plotted in linear intensity scale, smoothed by a Gaussian function of $1.5''$ FWHM and with a contrast adjustment to avoid the over-brightness of M87 nucleus and jets; (b) — the triple-ring feature (dashes) enhanced image with an unsharp mask. In the sharpened image, two rings (northwest ring 1 and southeast ring 2) are roughly along the M87 jet. The third ring 3 can be seen in broken segments, viz. the northern and southern portions fit in an ellipse with the M87 nucleus as its center. Ring 3 passes across eight bright X-ray knots identified by small open arrows.

reconstructed circular ring normal to the jet direction (if 43° to LOS) is 61° , 51° and 9° for ring 1, 2 and 3, respectively. This means that ring 3 is likely a circular ring nearly perpendicular to the M87 jet. For a jet orientation of 15° to the LOS, the corresponding angles Φ' of ring normal to the jet (see Table 1) are 55° , 33° and 22° , respectively. The derived values of Φ and Φ' for presumed ‘circular’ ring 1 and 2 are fairly large; these two rings might be elliptical in the 3-D space or their orientations are not perpendicular to the jet. Our estimate excludes the possibility that the elliptical shape of rings 1 and 2 is caused by relativistic projection effects if the two circular rings expand radially away from the jet axis while moving apart from each other relativistically along the line connecting the two ring centers, because by special relativity the ring would be elongated transverse to the jet direction. We note that ring 3 passes through eight X-ray bright knots with its center located exactly at the

M87 nucleus. The chance of such a coincidence is small.

As projected ring 1 and 2 roughly align along the direction of the M87 jet and counter jet, their intrinsic elliptical (instead of circular) shapes in 3-D space are plausible. Given relatively small angle of the ring 3 normal to the jet (9° or 22°), one may qualitatively regard ring 3 as circular and perpendicular to the jet.

4. SPECTROSCOPY OF THE THREE RINGS

From Figure 2, the softest regions locate at (i) around the jet within a $\sim 20''$ radius sector from west to north of the nucleus, (ii) an extended arc coincident with the east portion of ring 1 from north to south of the nucleus, (iii) a short arc coincident with ring 3 about $\sim 30''$ away from the nucleus in the northwest and (iv) some extended filaments southeast of the nucleus outside the three rings. By comparing Figure 2 with the $H\alpha + [N II]$ emissions of the central Virgo cluster (Sparks et al. 1993), we find that the soft region (i) and (iv) are correlated with $H\alpha + [N II]$ filaments. Similar correlations were also found in the Perseus cluster (Fabian et al. 2003b), indicating that intracluster gases become cooler when adjacent to the filaments due to thermal conduction.

The association of regions (ii) and (iii) with ring 1 and 3 respectively is interesting with region (ii) being more striking. A harder spectrum may correspond to a higher temperature. Different temperatures along ring 1 indicate that X-ray emissions may not be simply caused by a high density of electrons alone, but may involve supersonic shock flows from the AGN. Other parts of rings without temperature difference relative to surroundings might indicate subsonic flows.

Energy spectra are derived from two segments of ring 1, viz., the east part identified with region (ii) and the west part. To compare the spectra in these two parts with their environments, the source region is partitioned as an elliptical annulus along ring 1 with a width of $\sim 4''$ and a background region of a bigger elliptical annulus outside $5''$ of ring 1 with a width of $\sim 2''$. The source and background regions are separated into two parts by a straight solid line in Figure 2.

In Figure 2, the east part carries features, while the west part blends with the environment. We adopt a hot diffuse gas emission model (VMEKAL) to fit the spectra of both parts, with free parameters of equivalent hydrogen column, temperature and elemental abundances of O, Ne, Mg, Si, S and Fe. The fitting is carried out using *XSPEC* 11.3. The best-fit temperatures are $0.74^{+0.04}_{-0.05}$ keV ($\chi^2/\text{d.o.f.} = 71/54$) for the east part and $1.32^{+0.04}_{-0.05}$ keV ($\chi^2/\text{d.o.f.} = 53/55$) for the west part. A remarkable difference in plasma temperature can be seen from energy spectra using the hardness ratio map in Figure 2. In contrast, only the central ring of SN1987A can be resolved by *Chandra* using a sub-pixel technique (Burrows et al. 2000; Park et al. 2002; Michael et al. 2002). As its X-ray spectrum may be fit by a plane-parallel shock model, the central ring of SN1987A is thought to involve an expanding blast wave. By this clue, we attempt to fit the spectra of both east and west parts of ring 1 (Figure 1b) using the plane-parallel shock model (VPSHOCK) with the same free parameters of elemental abundance indicated above. The west part spectrum does not fit the plane-parallel model well with a large $\chi^2/\text{d.o.f.} \sim 5$, while the east part spectrum fits well with the shock model. The best-fit

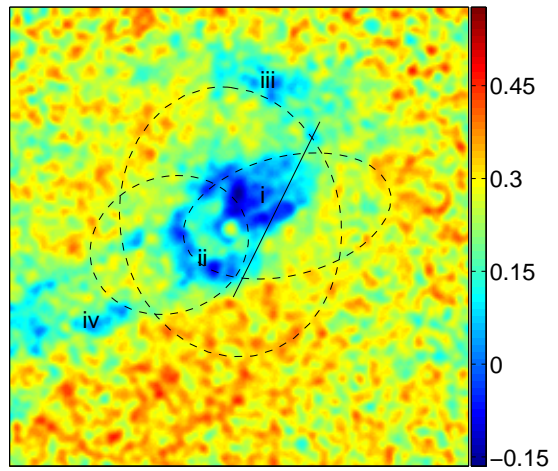


FIG. 2.— Hardness ratio map in the central Virgo cluster. The two energy bands are 0.5–1.0 keV and 1.0–2.5 keV. Each pixel stands for $H = (c_2 - c_1)/(c_2 + c_1)$ where c_1 and c_2 are photon counts at this pixel in the lower and higher energy bands respectively. Four softest regions are labeled. The solid line indicates a separation of the two parts along ring 1 for spectral comparisons (see § 4).

temperature is $0.71^{+0.04}_{-0.04}$ keV ($\chi^2/\text{d.o.f.} = 77/53$), consistent with the hot plasma model. This suggests that ring 1 may involve a blast wave where the west part might have been thermalized with the surroundings and the east part might be in the process of being thermalized. For the east part, the best-fit abundances of elements O, Si, S, and Fe in the thermal model are systematically lower than that in the west part. The enhancement of abundances in the warmer region may indicate more active nuclear processes in the past, perhaps caused by the thermalization in the west part. The similar temperature-abundance correlation is also found with *XMM* in the inner region for radius $\lesssim 1'$ (Böhringer et al. 2001) and for the two large-scale arms (Belsole et al. 2001). Because of uncertainties in estimating abundances with *Chandra* data for the fine structures, we refrain from more detailed comparisons with previous results of *XMM* for the larger structures.

5. DISCUSSIONS

The triple-ring pattern revealed in the central Virgo cluster is the only one observed since the discovery of triple rings in SN1987A⁸ (Burrows 1995). The ring sizes in the Virgo cluster are several thousand times larger than those of SN1987A. The triple-ring structure of SN1987A has been simulated in terms of interacting winds near the end of stellar evolution. According to Tanaka & Washimi (2002), during the star's red supergiant phase, slower winds persist. Prior to the supernova explosion, the red supergiant somehow evolved into a blue supergiant that drove faster winds. Magnetohydrodynamic (MHD) interactions of fast and slow winds from a rotating star produce the triple-ring structure in SN1987A. We suspect that a triple-ring structure might be generic in a rotating system involving magnetized faster winds catching up slower winds (Lou 1994, 1996). Meanwhile a central source of radiation is required for the rings to shine in the X-ray band. For SN1987A,

⁸ http://oposite.stsci.edu/pubinfo/jpeg/SN1987A_Rings.jpg

the strong UV radiation from the supernova provides the necessary illumination.

We suspect that a catastrophic merging event around the M87 nucleus might be responsible for the triple-ring structure revealed here. Merging of two SMBH systems has been proposed to drive the observed X-shaped radio lobes (Merritt & Ekers 2002). In this scenario, a ‘slower wind’ was present before the merging begins, e.g., a mixture of galactic winds from two merging galaxies. A ‘faster wind’ was then driven during the merging process. It has been suggested that an active AGN phase occurred in the core region of M87 at about 10^8 years ago (Kaiser 2003); perhaps, this AGN was triggered by the merging event discussed above, when significantly higher accretion rate was provided by the merger. The merger may fuel both the radiation energy output of the AGN and the growth of the supermassive black hole in the center; huge amount of high energy radiation shines the triple rings in X-ray bands. It is also plausible that the resulting SMBH spins rapidly to power the highly collimated M87 jets (Blandford & Znajek 1977).

F04 revealed two expanding cavities around the M87 jet and counter jet, enclosed within our ring 1 and 2 respectively. By different external pressures, they inferred the far front of the cavities is mildly supersonic while the inner part, close to the nucleus, is collapsing. We suggest that these two rings are actual rings instead of projections of prolate spheroids, because when two cavities collide into each other it is hard to maintain their spherical shapes in the spatially overlapping portions of the two spheroids, and consequently their projections cannot be viewed as two complete and nested rings. We further suggest that when the jets form, they push materials around and drive powerful blast waves of ring shapes.

Qualitatively similar central structures are present in the clusters Perseus (Fabian et al. 2003a), Hydra A (McNamara et al. 2001), Centaurus A (Kraft et al. 2002; Karovska et al. 2002) and Virgo (F04). Physically, core activities can excite large-scale acoustic waves (p -modes) and internal gravity waves (g -modes) in a deep gravitational potential well of central galaxy cluster (Lou 1995). Cluster core activities can be either violent and sporadic or sustained at a level or a combination of

both. Depending on the phase of acoustic wave propagation and on physical properties of core environment, we may observe various X-ray morphologies superposed onto a smooth luminous core. Beautiful acoustic rings or arcs have been revealed in Perseus (Fabian et al. 2003a) and in Virgo on larger scales (F04). Intense core X-ray emissions tend to induce inflows of gas that perturb the dark matter via gravity. The violent relaxation proceeds in a sound-crossing timescale (Lynden-Bell 1967). This could be a persistent source of p -modes and g -modes in a cluster core. By such wave and Landau-damping processes, slowly inward drifting gas and dark matter are virialized to sustain X-ray losses from hot electron gas. As a cluster core may involve magnetic field of strengths up to $\sim 30 - 40 \mu\text{G}$, MHD waves should also play significant roles. Based on the hardness ratio map and the energy spectra fitting, we infer only parts of ring 1 and 3 involve supersonic shock flows and are in processes of being thermalized with the surroundings. By this reasoning, other parts without apparent difference with surroundings might have been thermalized already. In summary, we hope that the triple-ring structure of M87 in the central Virgo cluster would stimulate more theoretical, simulation and observational studies of MHD flow, wave and shock interactions.

We thank the anonymous referee whose insightful and instructive comments have improved our work significantly. This work was supported in part by the Special Funds for Major State Basic Science Research Projects, by the Directional Research Project on High Energy Astrophysics of the Chinese Academy of Sciences, and by the National Natural Science Foundation of China (NSFC) grants No. 10233030, 10028306 and 10373009. SNZ also acknowledges supports by NASA’s Marshall Space Flight Center and by NASA’s Long Term Space Astrophysics Program. YQL also acknowledges partial support by the ASCI Center for Astrophysical Thermonuclear Flashes at the U. of Chicago under DOE contract B341495, and by the Yangtze Endowment from the MOE through the Tsinghua Univ. The data were taken from the HEASARC online service of the NASA/GSFC.

REFERENCES

- Begelman, M. C. 2003, *Science*, 300, 1898
 Belsole, E. et al. 2001, *A&A*, 365, L188
 Biretta, J. A., Zhou, F., & Owen, F. N. 1995, *ApJ*, 447, 582
 Biretta, J. A. et al. 1999, *ApJ*, 520, 621
 Blandford, R. D., & Znajek, R. L. 1977, *MNRAS*, 179, 433
 Böhringer, H. et al. 2001, *A&A*, 365, L181
 Burrows, C. J. 1995, *ApJ*, 452, 680
 Burrows, D. N. et al. 2000, *ApJ*, 543, L149
 Fabian, A. C. et al. 2003a, *MNRAS*, 344, L43
 Fabian, A. C. et al. 2003b, *MNRAS*, 344, L48
 Fan, Z. H., & Lou, Y. Q. 1996, *Nature*, 383, 800
 Feng, H. et al. 2002, *GRL*, 29(3), doi: 10.1029/2001GL013992
 Fishman, G. J. et al. 1994, *Science*, 264, 1313
 Forman, W. et al. 2004, *ApJ*, submitted (astro-ph/0312576, F04)
 Goldreich, P., & Tremaine, S. 1978, *Icarus*, 34, 240
 Haisch, B., Strong, K. T., & Rodono, M. 1991, *ARA&A*, 29, 275
 Hines, D. C., Owen, F. N., & Eilek, J. A. 1989, *ApJ*, 347, 713
 Kraft, R. P. et al. 2002, *ApJ*, 569, 54
 Kaiser, C. R. 2003, *MNRAS*, 343, 1319
 Karovska, M. et al. 2002, *ApJ*, 577, 114
 Li, T. P. 2001, *Chinese J. Astron. Astrophys.*, 1, 313
 Lin, C. C., & Shu, F. H. 1964, *ApJ*, 140, 646
 Lou, Y. Q. 1994, *J. Geophys. Res.*, 99, 8491
 Lou, Y. Q. 1995, *MNRAS*, 276, 769
 Lou, Y. Q. 1996, *MNRAS*, 279, 129
 Lou, Y. Q., & Fan, Z. H. 1998, *ApJ*, 574, 102
 Lynden-Bell, D. 1967, *MNRAS*, 136, 101
 McNamara, B. R. et al. 2001, *ApJ*, 534, L135
 Merritt, D., & Ekers, R. D. 2002, *Science*, 297, 1310
 Mészáros, P. 2001, *Science*, 291, 79
 Michael, E. et al. 2002, *ApJ*, 574, 166
 Mirabel, I. F., & Rodríguez, L. F. 1999, *ARA&A*, 37, 409
 Park, S. et al. 2002, *ApJ*, 567, 314
 Ray, T. P. et al. 1996, *ApJ*, 468, L103
 Sparks, W. B., Ford, H. C., & Kinney, A. L. 1993, *ApJ*, 413, 531
 Tanaka, T., & Washimi, H. 2002, *Science*, 296, 321
 Whitmore, B. C. et al. 1995, *ApJ*, 454, L73
 Young, A. J., Wilson, A. S., & Mundell, C. G. 2002, *ApJ*, 579, 560
 Zhang, S. N. et al. 2000, *Science*, 287, 1239